

New Phosphors for white LEDs: *Material Design Concepts*

M Mikami, H Watanabe, K Uheda, S Shimooka, Y Shimomura, T Kurushima,
and N Kijima

Mitsubishi Chemical Group Science and Technology Research Center, Inc.,

1000, Kamoshida-cho, Aoba-ku, Yokohama, 227-8502, Japan

E-mail: mikami.masayoshi@mv.m-kagaku.co.jp

Abstract. Efficient phosphors for white LEDs have been successfully developed, wherein some *Material Design Concepts* were utilized to promote our research and development effectively and efficiently. Useful ideas for the development of our red and green phosphors, Sr-rich (Sr,Ca,Eu)AlSiN₃, (Ba,Eu)₃Si₆O₁₂N₂ and (Ca,Ce)₃(Sc,Mg)₂Si₃O₁₂, are reviewed.

1. Introduction

White LED is highly expected as one of the most promising eco-friendly light sources, with much less energy consumption (less CO₂ gas exhaustion) than conventional light sources such as incandescent lamp. In most white LED devices, phosphors doped with rare earth elements such as Ce³⁺/Eu²⁺ are excited by blue InGaN LED chip and emit longer-wavelength light, and the mixing of the resultant light with the remains of the pump light composes desired white colour [1]. Although the combination of blue InGaN LED chip and yellow phosphor (Y,Ce)₃Al₅O₁₂ has been the most popular on the market, the share of green and red phosphors has been steadily increasing for high colour rendering index and good colour reproducibility for general lighting and liquid crystal display (LCD) backlight in cell phone and flat panel display. Thus the competition for new green/red phosphors has been more and more intensive all over the world. It is desired to swiftly develop new green/red phosphors with sufficient chemical durability and ideal luminescent properties (emission peak wavelength, emission spectrum width, excitation spectra excitable by blue light, and high efficiency at high temperature of 80-150°C and so forth). For Ce³⁺/Eu²⁺-doped phosphors that utilize 5d-4f transition for light emission, it is significant to design ligand as well as host for efficient luminescence under high temperature.

We have successfully developed new red and green phosphors, Sr-rich (Sr,Ca,Eu)AlSiN₃ [2,3], (Ba,Eu)₃Si₆O₁₂N₂ [4,5] and (Ca,Ce)₃(Sc,Mg)₂Si₃O₁₂ [6], by close collaboration between experiment and theory. In this paper, we present how our phosphors have been speedily developed by applying *Material Design Concepts*. Since we reported the synthesis methods and the optical properties of the phosphors in detail elsewhere [2-6], we will overview useful theoretical/empirical ideas in the research and development (R&D); specifically, some crystal rules to understand host structures, empirical rules for 4f-5d transition of Ce³⁺/Eu²⁺ in solids, and some rules of thumb for doping will be stressed.

2. (Sr,Ca,Eu)AlSiN₃ : red phosphor

Nitridoaluminosilicate CaAlSiN₃ and its derivatives have attracted more and more attention owing to the fact that the material doped with rare-earth element exhibits efficient luminescence under blue or

Near-UV(NUV) InGaN diode irradiation. For example, a red phosphor, Eu^{2+} -doped CaAlSiN_3 , with emission peak of 650nm with full-width-half-maximum (FWHM) of about 90 nm, has small thermal quenching of luminescence and sufficient chemical durability for white LED use [7,8]. Typical photoluminescence (PL) and photoluminescence excitation (PLE) spectra of $(\text{Ca},\text{Eu})\text{AlSiN}_3$ are shown in figure 1. This red phosphor appears useful for LCD backlight as well as general lighting. The crystal structure of CaAlSiN_3 can be regarded as distorted AlN-based wurtzite superstructure ($Cmc2_1$) with four-coordinated Al and Si disordered on $8b$ site and five-coordinated Ca occupying $4a$ site. The structural features such as inevitable Al/Si random distribution can be well understood from Pauling’s second crystal rule and first-principles calculation based on density functional theory (DFT) [9]. The wideness of absorption/emission may be related to the non-uniformity due to the Al/Si random distribution (i.e. inhomogeneous broadening) as suggested in Ref. [7].

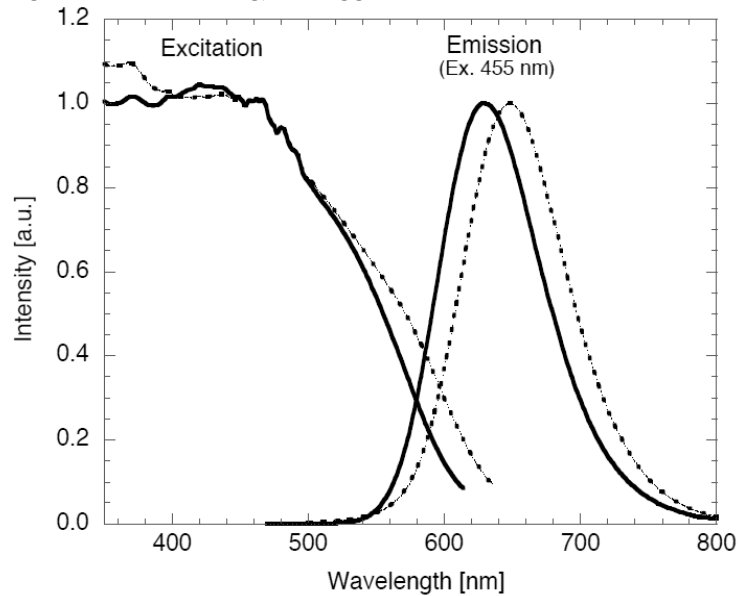


Figure 1. Normalized Photoluminescence and Photoluminescence excitation spectra of $(\text{Ca},\text{Eu})\text{AlSiN}_3$ (dotted lines) and $(\text{Sr},\text{Ca}, \text{Eu})\text{AlSiN}_3$ (solid lines).

Since the colour of $(\text{Ca},\text{Eu})\text{AlSiN}_3$ is somewhat deep red for some kinds of general lighting purposes, it is desirable to tune the red emission to orange-reddish colour without loss of the quantum output. For this purpose, it is natural to think of tuning the ligand field around the Eu^{2+} site. Here we refer to the empirical equation devised by Dorenbos, wherein Eu^{2+} 4f-5d absorption/emission energy in inorganic compound A ($E_{\text{abs}}(\text{Eu}^{2+}, A)$ and $E_{\text{em}}(\text{Eu}^{2+}, A)$, respectively) are expressed as follows [10,11] (figure 2):

$$E_{\text{abs}}(\text{Eu}^{2+}, A) = E_{\text{FreeA}}(\text{Eu}^{2+}) - D(2+, A) \quad (1)$$

$$\begin{aligned} D(2+, A) &= \varepsilon_c(2+, A) + \varepsilon_{\text{cfs}}(2+)/r(A) \\ &= 0.64 \cdot D(3+, A) - 0.233 \\ &= 0.64 \cdot (\varepsilon_c(3+, A) + \varepsilon_{\text{cfs}}(3+)/r(A) - 0.234) - 0.233 \text{ (eV)} \end{aligned} \quad (2)$$

$$E_{\text{em}}(\text{Eu}^{2+}, A) = E_{\text{abs}}(\text{Eu}^{2+}, A) - \Delta S \quad (3)$$

where $E_{\text{FreeA}}(\text{Eu}^{2+})$ is the 4f-5d transition energy for the free gaseous ion and is rounded to $34\,000 \text{ cm}^{-1}$; the redshift $D(2+, A)$ ($D(3+, A)$) is defined as the energy of $4f^{n-1}5d$ -levels of a $2+(3+)$ lanthanide ion in compound A relative to the level energies in the free ion; ε_c is the downward shift of the average energy of the five 5d levels of the rare earth element relative to the free ion case (so-called, centroid shift); ε_{cfs} is the difference between the energy of the lowest and highest 5d level (so-called, crystal field splitting); $r(A)$ is the fraction of ε_{cfs} that contributes to the redshift; ΔS denotes Stokes shift. This concept holds true with Ce^{3+} 4f-5d transition as well [12]. The centroid shift (ε_c) is commonly associated with the nephelauxetic effect which is often attributed to the covalency between the 5d

orbital of the luminescent centre and the p orbital of the ligand anion, parameterized with *spectroscopic* polarizabilities. According to Dorenbos, *spectroscopic* polarizability is correlated with atomic polarizability (or electronegativity) of anions [13], which contributes to optical dielectric tensors or refractive indices. The crystal field splitting (ϵ_{cfs}) is determined by the shape and size of the first anion coordination polyhedron. On the basis of this concept, we can expect that derivatives of CaAlSiN_3 may have different kinds of red colour emissions for Eu^{2+} dopant. Specifically, the emission peak of Sr-rich (Sr, Ca, Eu) AlSiN_3 will shift to orange-red owing to the weaker crystal splitting field induced by the enlargement of the crystal lattice of (Sr,Ca,Eu) AlSiN_3 ; note that the ionic radius of Ca^{2+} (Sr^{2+}) is 114 pm (132 pm) for six coordinates.

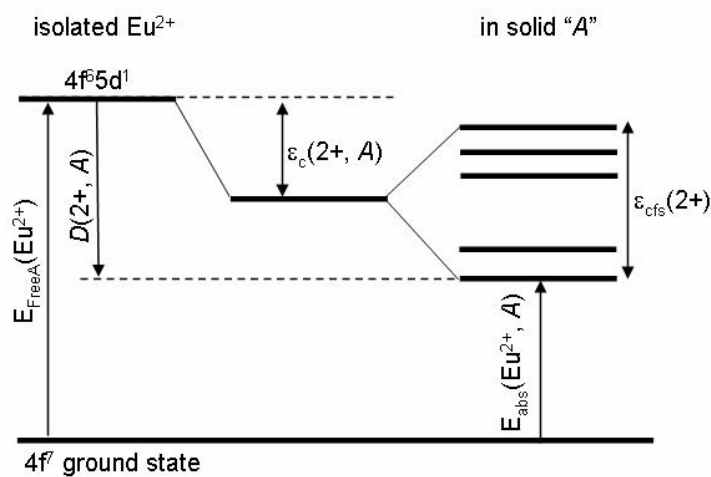


Figure 2. Schematic representation of the influence of the environment of a Eu^{2+} ion on the positions of electronic states. The centroid shift $\epsilon_c(2+, A)$, crystal field splitting $\epsilon_{\text{cfs}}(2+)$, redshift $D(2+, A)$, and the lowest energy 4f-5d transition of Eu^{2+} $E_{\text{abs}}(\text{Eu}^{2+}, A)$ are indicated.

Through our intensive R&D on (Sr,Ca,Eu) AlSiN_3 , we realized that the synthesis feasibility of the Sr-rich phase was intrinsically different from the case of (Ca,Eu) AlSiN_3 . Single phase of (Ca,Eu) AlSiN_3 can be synthesized by conventional solid state reactions of the nitride starting materials under N_2 pressure of about 1 MPa [7,8]. On the other hand, the synthesis of single phase of Sr-rich (Sr, Ca,Eu) AlSiN_3 had been practically difficult under the similar experimental conditions; substantial amount of (Sr,Ca,Eu) $_2\text{Si}_5\text{N}_8$ and AlN were inevitable. The unwanted phase such as (Sr,Ca,Eu) $_2\text{Si}_5\text{N}_8$ must be avoided because of possible patent issues. After trials and errors, we finally synthesized single phase of Sr-rich (Sr,Ca,Eu) AlSiN_3 by direct nitridation of (Sr,Ca,Eu)AlSi alloy powder under the high pressure of 190 MPa in a hot isostatic pressing process [2,3]. The PL and PLE spectra of (Sr,Ca,Eu) AlSiN_3 is shown in figure 1. We have successfully shift the colour spectrum of (Sr,Ca,Eu) AlSiN_3 to the orange-red region, with the peak position of 628nm without any loss of the other physical/optical properties. Still, we needed to understand the mechanism of the tricky synthesis of (Sr,Ca,Eu) AlSiN_3 .

To clarify the reason, first-principles calculation of $M\text{AlSiN}_3$ (M : alkaline-earth element) was performed on the basis of density functional theory (DFT) [14]. We noticed that the optimized crystal structure of SrAlSiN_3 appears more distorted than that of CaAlSiN_3 [15]; this picture on the crystal structure has been experimentally confirmed from the recent Rietveld analysis on (Sr, Eu) AlSiN_3 [16]. Moreover, the calculation revealed that the rate limiting reaction step $M\text{SiN}_2 + \text{AlN} \rightarrow M\text{AlSiN}_3$ is exothermic for $M=\text{Ca}$ (-4 kcal/mol) and endothermic for $M=\text{Sr}$ (+1 kcal/mol), respectively [15]. This may be related with the distorted crystal structure of SrAlSiN_3 as stated in the above. It is also noted that typical side reactions, $2M\text{SiN}_2 + \text{Si}_3\text{N}_4 \rightarrow M_2\text{Si}_5\text{N}_8$, are exothermic: -10 kcal/mol for $M=\text{Ca}$, and

-20 kcal/mol for $M=\text{Sr}$, respectively [15]. Thus SrSiN_2 may prefer the reaction with Si_3N_4 leading to $\text{Sr}_2\text{Si}_5\text{N}_8$ generation with starting-material AlN left non-reacted, rather than generation of SrAlSiN_3 . Therefore, it is essentially important to change the chemical reaction path to obtain single phase of Sr-rich $(\text{Sr,Ca,Eu})\text{AlSiN}_3$.

We also realized the meaning of the high pressure of nitrogen gas, which can work for the stability of $(\text{Sr,Ca,Eu})\text{AlSiN}_3$ against $(\text{Sr,Ca,Eu})_2\text{Si}_5\text{N}_8$ and AlN ; under sufficiently high chemical potential of nitrogen potential ($\mu(\text{N})$), the chemical potential of $M\text{AlSiN}_3$ can be more stable than the sum of the chemical potentials of $(\text{Sr,Ca,Eu})_2\text{Si}_5\text{N}_8$, AlN , alkaline earth element M and nitrogen: namely, $5\mu(M\text{AlSiN}_3) < \mu(M_2\text{Si}_5\text{N}_8) + 5\mu(\text{AlN}) + 3\mu(M) + 2\mu(\text{N})$. The higher pressure of nitrogen (less stable $\mu(\text{N})$) is necessary for the synthesis of $(\text{Sr,Ca,Eu})\text{AlSiN}_3$, because $\mu((\text{Sr,Ca,Eu})\text{AlSiN}_3)$ is less stable than $\mu((\text{Ca,Eu})\text{AlSiN}_3)$ presumably due to the larger crystal distortion induced by much Sr-content.

It is interestingly noted that the first-principles calculation of $(\text{Sr,Ca})\text{AlSiN}_3$ solid solution gave some hints on experimental results on lattice constants of $(\text{Sr,Ca})\text{AlSiN}_3$ [15]. Although the calculated lattice constants appeared qualitatively good agreement with the experimental results [2,3], somewhat quantitative disagreement remained. In particular, the calculated a -axis monotonically increased with Sr-content, whereas the experimental a -axis did not increase. Still, our computations on solid solution of $M\text{AlSiN}_3\text{-Si}_2\text{N}_2\text{O}$ suggested that vacancies of alkaline earth elements can induce such deviation between experiment and theory [15]. In fact, our chemical analysis indicated the deficiency of Sr/Ca from the stoichiometrical composition. Thus the experiment and the theory have compensated each other to have common picture of the microscopic crystal models for our $(\text{Sr,Ca,Eu})\text{AlSiN}_3$ samples.

In this way, the first-principles calculation gave the specific picture of atomic/electronic structure of SrAlSiN_3 to understand the experimental results on Sr-rich $(\text{Sr,Ca,Eu})\text{AlSiN}_3$. The understanding based on thermodynamics kept us from further efforts for the conventional solid state reactions of $(\text{Sr,Ca,Eu})\text{AlSiN}_3$, so that we concentrated on the new nitridation method of $(\text{Sr,Ca,Eu})\text{AlSi}$ alloy. Our R&D had been thus promoted by the close collaboration between experiment and theory.

3. $(\text{Ba,Eu})_3\text{Si}_6\text{O}_{12}\text{N}_2$: green phosphor

During quest for new oxynitrides in the phase diagram of $\text{BaO-SiO}_2\text{-Si}_3\text{N}_4$, we have successfully synthesized a new oxonitridosilicate phosphor, $(\text{Ba,Eu})_3\text{Si}_6\text{O}_{12}\text{N}_2$ [4]. It is interestingly noted that our finding has completed a series of compounds, $\text{Ba}_3\text{Si}_6\text{O}_{15-3x}\text{N}_{2x}$ ($x=0, 1, 2,$ and 3): BaSi_2O_5 (Sanbornite), $\text{Ba}_3\text{Si}_6\text{O}_{12}\text{N}_2$ (our work), $\text{Ba}_3\text{Si}_6\text{O}_9\text{N}_4$ [17], and $\text{BaSi}_2\text{O}_2\text{N}_2$ [18,19], respectively. Figure 3 shows PL and PLE spectra of $(\text{Ba,Eu})_3\text{Si}_6\text{O}_{12}\text{N}_2$. $(\text{Ba,Eu})_3\text{Si}_6\text{O}_{12}\text{N}_2$ has an efficient green emission under blue or NUV LED light. The broad excitation band observed from 250 nm to 500 nm is assigned to the allowed transition from $4f^7$ ground state to $4f^65d$ state of Eu^{2+} . On the other hand, green emission spectrum with rather narrow FWHM of 68 nm is observed around 525 nm due to the $5d-4f$ transition of Eu^{2+} . This compound appears promising green phosphor for applied to LCD backlight owing to high colour purity (the CIE colour coordinates (0.28, 0.64)) and small thermal quenching. Incidentally, $(\text{Ba,Eu})_3\text{Si}_6\text{O}_{12}\text{N}_2$ exhibits much smaller thermal quenching of luminescence than another popular green phosphor $(\text{Ba,Sr,Eu})_2\text{SiO}_4$ [20]; the emission intensity of $(\text{Ba,Eu})_3\text{Si}_6\text{O}_{12}\text{N}_2$ at 100°C was about 90% of that measured at room temperature (R.T.), whereas the emission intensity of $(\text{Ba,Sr,Eu})_2\text{SiO}_4$ at 100°C was about 75% of that at R.T. [4].

Although we had not grasped the exact phase at the early stage of R&D, we finally identified the crystal structure by a new protocol combining X-ray/neutron powder diffraction analysis with first-principles study [4,5]. First, an almost single phase of the new compound was prepared by conventional solid state reaction. The X-ray diffraction (XRD) indicated that the compound should be a new crystal phase. The crystal symmetry (trigonal) and approximate lattice constants ($a=7.48(1)\text{\AA}$, $c=6.47(1)\text{\AA}$) were obtained by TEM. Considering chemical analysis indicating oxygen-rich oxynitride phase and weight density ($\rho = 4.13 \text{ g/cm}^3$) indicating $Z=1$, we assumed that the compound has crystal structure close to $\text{Ba}_3\text{Si}_6\text{O}_9\text{N}_4$ ($P3$, $a = 7.249(1)\text{\AA}$, $c = 6.784(2)\text{\AA}$, $Z=1$, $\rho = 4.199 \text{ g/cm}^3$) [17]. Judging from the trigonal symmetry along with crystal rules as described later, we assume a plausible chemical formula as $\text{Ba}_3\text{Si}_6\text{O}_a\text{N}_b$. Simple mathematics based on the charge neutrality led to $a=15-3x$ and $b=2x$.

Among possible compositions, $\text{Ba}_3\text{Si}_6\text{O}_{15-3x}\text{N}_{2x}$ ($x = 0, 1, 2, 3$), only $\text{Ba}_3\text{Si}_6\text{O}_{12}\text{N}_2$ ($x=1$) had not been reported by that time. Thus the crystal structure of $\text{Ba}_3\text{Si}_6\text{O}_{12}\text{N}_2$ was approximately solved as $P3$ by a direct method (EXPO program [21]) from the XRD. The geometry was then optimized by first-principles calculation based on DFT [14]. It turned out that the calculated geometry has inversion symmetry, which could not be easily identified only by the XRD analysis. The optimized crystal structure was used as initial inputs for Rietveld analysis of the X-ray/neutron diffraction. All of the crystallographic parameters were refined by RIETAN-2000 program [22], and then the structure was finally determined as $P\bar{3}$. The identification of the exact chemical composition and crystal structure helped us to improve the physical/optical properties of the phosphor as single phase.

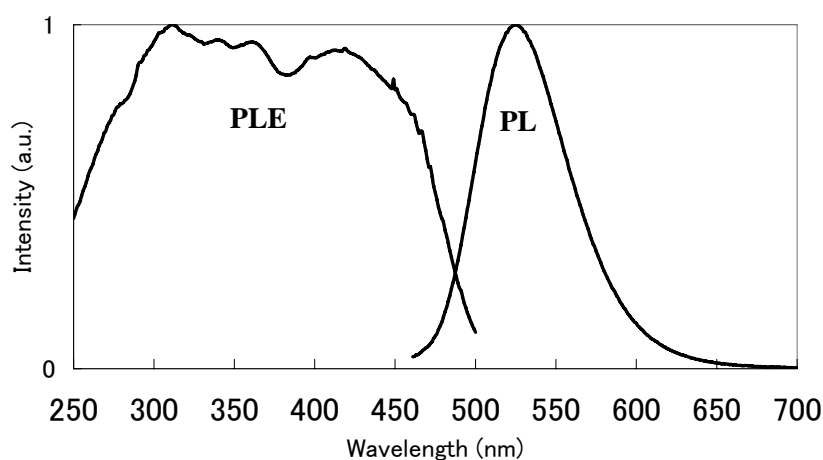


Figure 3. Normalized photoluminescence and photoluminescence excitation spectra of $(\text{Ba,Eu})_3\text{Si}_6\text{O}_{12}\text{N}_2$.

Incidentally, we refer to a useful crystal rule that helped us during the above identification process. The bond-number equality concept (BNEC) [23] can give us the information on the coordination in ionic compounds such as nitridosilicates. The BNEC utilizes the fact that the number of bonds originating from four-coordinated silicon ($\text{Si}^{[4]}$) must be equal to the number of bonds originating from nitrogen atoms ($\text{N}^{[1]}$, $\text{N}^{[2]}$, $\text{N}^{[3]}$, and $\text{N}^{[4]}$). Here the superscript with square brackets denotes the coordination number of atom. We notice that the BNEC implies “8–N rule”[24] by the combination with the charge neutrality in chemical formula. Specifically, in alkaline-earth nitridosilicates, nitrogen $\text{N}^{[2]}$ ($\text{N}^{[1]}$) may be considered as one(two)-electron reservoir to compensate electrons from alkaline earth elements; for example, $\text{Ca}_2\text{Si}_5\text{N}_8$ can be expressed as $\text{Ca}_2\text{Si}_5^{[4]}\text{N}_4^{[2]}\text{N}_4^{[3]}$ [23] wherein the number of $\text{N}^{[2]}$ equals with the twice of the number of calcium atoms. To find a natural extension of the BNEC for oxynitrides, we examined crystal structures of $(M,\text{Eu})_3\text{Si}_6\text{O}_{15-3x}\text{N}_{2x}$ ($x = 2$ and 3) and confirmed $\text{Ba}_3\text{Si}_6^{[4]}\text{O}_6^{[1]}\text{O}_3^{[2]}\text{N}_4^{[3]}$ / $\text{Eu}_3\text{Si}_6^{[4]}\text{O}_6^{[1]}\text{O}_3^{[2]}\text{N}_4^{[3]}$ (built up of corner-sharing SiO_2N_2 tetrahedra)[17] and $\text{Ca}_3\text{Si}_6^{[4]}\text{O}_6^{[1]}\text{N}_6^{[3]}$ [25] / $\text{Eu}_3\text{Si}_6^{[4]}\text{O}_6^{[1]}\text{N}_6^{[3]}$ [26] (built up of corner-sharing SiON_3 tetrahedra), respectively. This observation implies that (oxygen-rich) oxynitrides favour $\text{N}^{[3]}$ rather than $\text{N}^{[1]}$ / $\text{N}^{[2]}$ and that only $\text{O}^{[1]}$ will work as electron reservoir for electrons released from alkaline earth elements or europium; the unsaturated bonds of $\text{N}^{[3]}$ ($\text{O}^{[2]}$) coordinate with three (two) silicon atoms; this may be related to the fact that nitrogen has more covalent (less ionic) character than oxygen. Then we confirmed that our compound can be certainly expressed as $\text{Ba}_3\text{Si}_6^{[4]}\text{O}_6^{[1]}\text{O}_6^{[2]}\text{N}_2^{[3]}$ (built up of corner-sharing SiO_3N tetrahedral). Incidentally, the recent crystal structure determination of $\text{BaSi}_2\text{O}_2\text{N}_2$ and $\text{SrSi}_2\text{O}_2\text{N}_2$

indicates that these oxynitrides also follow the crystal rule on the combination $N^{[3]}/O^{[1]}/O^{[2]}$, i.e. $Ba_3Si_6^{[4]}O_6^{[1]}N_6^{[3]}$ [18] and $Sr_3Si_6^{[4]}O_6^{[1]}N_6^{[3]}$ [27]. Hence, our crystal rule on $N^{[3]}/O^{[1]}/O^{[2]}$ along with Pauling’s crystal rules appears powerful to assume plausible crystal models (or exclude unrealistic crystal models) for oxynitrides. It can also be helpful to formulate possible crystal chemical formulae for the anion complexes of new oxynitrides.

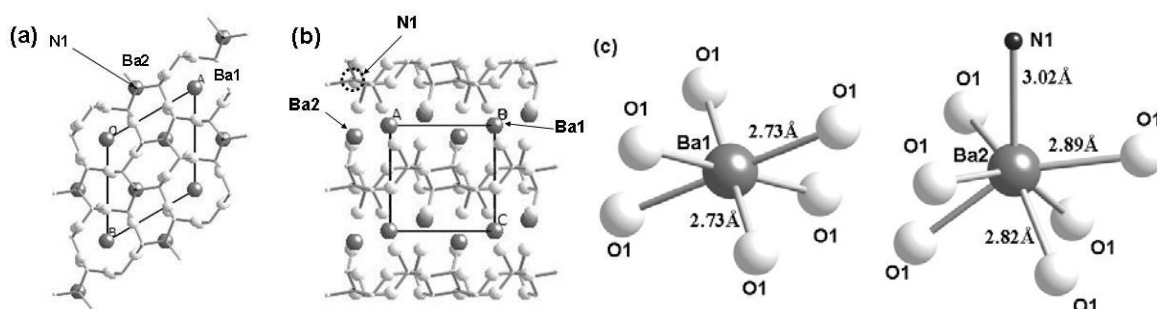


Figure 4. Projections of the unit cell of $Ba_3Si_6O_{12}N_2$ viewed along the c axis (a) and the b axis (b), and two coordination environments around Ba^{2+} ion (c); the clusters are defined within 3.2 Å.

Now we explain the crystal structure of $Ba_3Si_6O_{12}N_2$ in detail. It is illustrated in figure 4. The experimental and theoretical crystallographic data are summarized in table 1. The calculated lattice constants somewhat overestimate the experimental data due to the generalized-gradient approximation (GGA) in the DFT; the deviation appears within typical computational errors in GGA. The crystal structure has fused rings-sheets, $\infty [(Si_6^{[4]}O_6^{[2]}N_2^{[3]})O_6^{[1]}]^{6-}$, composed of eight-membered Si-(O,N) and twelve-membered Si-O rings. The compound is built up of corner sharing SiO_3N tetrahedra forming corrugated layers between which the Ba^{2+} ions are located. The Ba^{2+} ions occupy two different crystallographic sites; one is trigonal anti-prism (distorted octahedron) with six oxygen atoms (Ba1 site in figure 4(c)), and the other is trigonal anti-prism with six oxygen atoms, which is further capped with one nitrogen atom (Ba2 site in figure 4(d)).

Table 1. Crystallographic data of $Ba_3Si_6O_{12}N_2$ (experimental and theoretical data)

System (Space group)		Trigonal ($P\bar{3}$, No. 147)					
		Experiment (from XRD)			Theory		
Lattice parameters/Å		$a = 7.5046(8), c = 6.4703(5)$			$a = 7.59684, c = 6.57487$		
Atomic coordinates							
Label	Wyckoff-position	x	y	z	x	y	z
Ba1	1a	0	0	0	0	0	0
Ba2	2d	1/3	2/3	0.1039(2)	1/3	2/3	0.10060
Si1	6g	0.2366(6)	0.8310(6)	0.6212(8)	0.23594	0.82847	0.60978
N1	2d	1/3	2/3	0.568(3)	1/3	2/3	0.56311
O1	6g	0.356(2)	0.295(2)	0.173(1)	0.36096	0.29646	0.17190
O2	6g	0.000(1)	0.681(1)	0.589(2)	-0.01462	0.68138	0.58846

Although Eu^{2+} -dopant may occupy the both Ba^{2+} sites, the emission spectrum appears rather narrow just as only one kind of Eu^{2+} emits. This puzzling situation reminds us of apatite phosphors $(M, Eu)_5(PO_4)_3X$ (M : alkaline-earth element, X : halogen element) that can also emit rather narrow emission spectra, even though the crystal has two kinds of M sites where Eu^{2+} can occupy. Since the emission peak in the apatite depends on the species of X , the dominant Eu^{2+} emission band can be

assigned to the M site coordinated with oxygen and halogen atoms rather than the other crystallographic site coordinated with oxygen atoms only [28]. From this analogy, the narrow green emission in $(\text{Ba},\text{Eu})_3\text{Si}_6\text{O}_{12}\text{N}_2$ may be expected from the Ba2 site (coordinated with six oxygen atoms and one nitrogen atom), not the Ba1 site (with six oxygen atoms *only*). Indeed, the Eu^{2+} ion occupying the Ba2 site can have lower 5d-excited states due to the nitrogen ligand that has larger polarizability (covalency) than oxygen ligand so as to give larger centroid shift [13]. It may also be interesting to examine Eu^{2+} luminescence in other oxynitride $(M,\text{Eu})\text{Si}_2\text{O}_2\text{N}_2$ [29] from this viewpoint; the Ba-site in blue-green phosphor $(\text{Ba},\text{Eu})\text{Si}_2\text{O}_2\text{N}_2$ has cuboid-shaped ligand of eight oxygen atoms (defined within 3.2\AA), whereas the Sr(Ca)-site in green (yellow) phosphor $(\text{Sr},\text{Eu})\text{Si}_2\text{O}_2\text{N}_2$ ($(\text{Ca},\text{Eu})\text{Si}_2\text{O}_2\text{N}_2$) has distorted trigonal-prism-shaped ligand of six oxygen atoms that is further capped with one nitrogen atom (defined within 3.2\AA) [18].

It is also noteworthy that the optical properties of $(\text{Ba},\text{Eu})_3\text{Si}_6\text{O}_9\text{N}_4$ were quite different from $(\text{Ba},\text{Eu})_3\text{Si}_6\text{O}_{12}\text{N}_2$, although $\text{Ba}_3\text{Si}_6\text{O}_9\text{N}_4$ appears similar to $\text{Ba}_3\text{Si}_6\text{O}_{12}\text{N}_2$ from the viewpoint of crystal structure and chemical formula; $(\text{Ba},\text{Eu})_3\text{Si}_6\text{O}_9\text{N}_4$ exhibited blue-green PL with the peak about 480 nm only at low temperatures (little luminescence at R.T.), whereas $(\text{Ba},\text{Eu})_3\text{Si}_6\text{O}_{12}\text{N}_2$ exhibited intense green PL with the peak about 525nm at R.T. with thermal quenching smaller than $(\text{Ba},\text{Sr},\text{Eu})_2\text{SiO}_4$. Although the mechanism has not yet been fully understood, we may expect one possible explanation relying on the relative position of the Eu^{2+} 5d-excited states against the conduction band bottom/4f-ground states for the excitation/emission spectra and the thermal quenching [5]. In fact, the Ba-N bond in $\text{Ba}_3\text{Si}_6\text{O}_9\text{N}_4$ (about 3.2\AA) is longer than that in $\text{Ba}_3\text{Si}_6\text{O}_{12}\text{N}_2$ (about 3.0\AA), which may lead to the shorter wavelength of Eu^{2+} emission in $\text{Ba}_3\text{Si}_6\text{O}_9\text{N}_4$ due to smaller crystal field induced by the weak nitrogen coordination. The strong thermal quenching in $(\text{Ba},\text{Eu})_3\text{Si}_6\text{O}_9\text{N}_4$ may be ascribed to auto-ionization mechanism due to small gap between the Eu^{2+} excited states and the conduction band bottom of $\text{Ba}_3\text{Si}_6\text{O}_9\text{N}_4$. In fact, this is implied by our experiment on diffuse refractive spectra indicating the host absorption of $\text{Ba}_3\text{Si}_6\text{O}_9\text{N}_4$ is smaller than that of $\text{Ba}_3\text{Si}_6\text{O}_{12}\text{N}_2$. It also appears consistent with our band calculation (within GGA) indicating that $\text{Ba}_3\text{Si}_6\text{O}_9\text{N}_4$ may have smaller band gap than $\text{Ba}_3\text{Si}_6\text{O}_{12}\text{N}_2$: 4.37 eV for $\text{Ba}_3\text{Si}_6\text{O}_9\text{N}_4$ and 4.63 eV for $\text{Ba}_3\text{Si}_6\text{O}_{12}\text{N}_2$ [5]. Still, further experimental/theoretical investigations are awaited to fully understand the mechanism for such luminescent centres coordinated with multiple species of anions. This understanding could also lead to clear explanations to the similar phenomena of Ce^{3+} thermal quenching in some nitridosilicates [30].

4. $(\text{Ca},\text{Ce})_3(\text{Sc},\text{Mg})_2\text{Si}_3\text{O}_{12}$: green phosphor

A new garnet compound $(\text{Ca},\text{Ce})_3\text{Sc}_2\text{Si}_3\text{O}_{12}$ has been developed as a green phosphor excitable by the blue LED light and emits strong green light for white LEDs [31]. The X-ray absorption fine structure (XAFS) analysis indicated that the dopant Ce^{3+} occupies the eight-coordinated Ca^{2+} site rather than the six-coordinated Sc^{3+} [31]; note that the ionic radii of eight-coordinated Ce^{3+} and Ca^{2+} are 128.3pm and 126pm, whereas the ionic radii of six-coordinated Ce^{3+} and Sc^{3+} are 115pm and 88.5pm, respectively. The broad-banded luminescence of $(\text{Ca},\text{Ce})_3\text{Sc}_2\text{Si}_3\text{O}_{12}$ with peak wavelength of 505 nm (figure 5) exhibits the potential as a useful green phosphor for general lighting. It is also interestingly noted that the emission spectra is much shorter than yellow garnet-type phosphor $(\text{Y},\text{Ce})_3\text{Al}_5\text{O}_{12}$. The shorter luminescence in $(\text{Ca},\text{Ce})_3\text{Sc}_2\text{Si}_3\text{O}_{12}$ can be caused by weaker crystal field splitting or smaller centroid shift or the both; the weaker crystal field splitting may be related to longer lattice constant ($a=12.25\text{\AA}$ for $\text{Ca}_3\text{Sc}_2\text{Si}_3\text{O}_{12}$ in comparison with $a=12.01\text{\AA}$ for $\text{Y}_3\text{Al}_5\text{O}_{12}$) and/or small lattice distortion around Ce^{3+} [32], and the smaller centroid shift may be correlated with smaller refractive constant (1.78 for $\text{Ca}_3\text{Sc}_2\text{Si}_3\text{O}_{12}$, computed from Gladstone-Dale relation [33], in comparison with 1.83 for YAG), as implied in the equations (1) and (2).

It was expected that Ce^{3+} -doping at the Ca^{2+} site induced unintentional intrinsic/extrinsic defects such as Ca vacancy for the charge compensation. Since such intrinsic/extrinsic defects may limit the Ce^{3+} concentration automatically, we expected that the Ce^{3+} doping may be improved by co-doping at the Ca^{2+} or Sc^{3+} site. In practice, it was found that Mg co-doping at the Sc site increased the brightness of the phosphor [6]. The charge compensation for Ce^{3+} -dopant at the Ca^{2+} site by co-doping of Mg^{2+} at

the Sc^{3+} site appears plausible from the idea of Hume-Rothery solid-solution rules (or Darken-Gurry plot) about chemical similarity of elements [34]. The Darken-Gurry's rule states that doping may be feasible when the difference of ionic radii is within 15-20 % and the difference of electronegativity is less than about 0.4. In the case of ceramics compounds, the charge state of dopant should not be different from the substituted site by more than one [35]. With this in mind, we checked possible elements for the Ca-site and the Sc-site, and then noticed that Mg^{2+} (ionic radius: 86.0pm for six coordinates, electronegativity: 1.31) may substitute the Sc^{3+} site (ionic radius: 88.5pm for six coordinates, electronegativity: 1.36); note that Mg^{2+} size (ionic radius: 103 pm for eight coordinates) may be somewhat small to occupy the Ca^{2+} site (ionic radius: 126pm for eight-coordinates). Our chemical analysis based on inductively coupled plasma atomic emission spectrometer strongly suggested the above charge compensation mechanism; the Mg concentration almost corresponded to the charge compensation of Ce^{3+} doping at the Ca^{2+} site [6].

Incidentally, the photoluminescence spectra of the phosphors containing Mg were moved toward longer wavelengths with increasing Mg amount, as shown in figure 5. Appropriate amount of Mg brought 25% of increase in brightness of the phosphor. The spectral shift accompanied modification of decay characteristics, which revealed the appearance of another component of the luminescence. The modification was likely caused by the increase in amount of the Ce^{3+} activator due to Mg^{2+} co-doping. Interaction among the Ce^{3+} activators probably modified the luminescence characteristics [6].

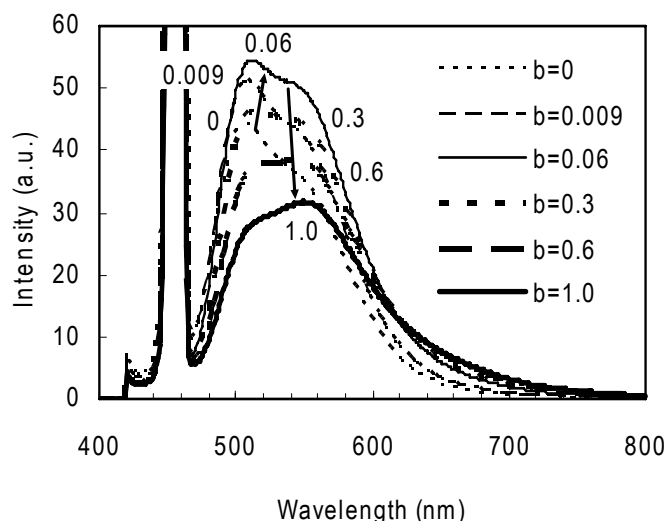


Figure 5. Photoluminescence spectra of $(\text{Ca,Ce})_3(\text{Sc,Mg})_2\text{Si}_3\text{O}_{12}$ phosphors under excitation at 455 nm. The compositions of materials were $(\text{Ca}_{2.97}\text{Ce}_{0.03})(\text{Sc}_{2-b}\text{Mg}_b)\text{Si}_3\text{O}_{12}$ ($0 \leq b \leq 1$).

5. Summary and Outlook

In this paper, we have reviewed some useful *Materials Design Concepts* for the development of the new phosphors; Dorenbos's empirical formula for the 4f-5d transitions in the rare-earth luminescent centres, thermodynamics for the synthesis feasibility, crystal rules such as bond number equality concept for plausible crystal modelling, and chemical similarity based on Darken-Gurry plot for effective co-doping. By applying the first-principles calculation effectively, we discussed reactivity among solid phases by computing heats of formation and pictured plausible crystal structure models, which gave us useful hints for the R&D. Incidentally, crystal modelling based on first-principles calculation may be useful for other cases such as silicate phosphors [36].

Still, unresolved issues lie ahead of us. It is desired to swiftly develop many kinds of phosphors with high quantum efficiency, desired colour spectra, little thermal quenching, sufficient chemical durability, and little photo-thermal degradation for long-life operation in white LED devices. Although we do not know how to theoretically predict the trend of durability/degradation before synthesis, we

might have possibilities to design efficient phosphors with desired colour and little thermal quenching by evaluating the excited states of rare-earth dopants and band structures of host materials much more quantitatively than ever. For multinary compounds such as oxynitride phosphors, methodology beyond crystal field theory is definitely necessary. To our best knowledge, there are few discussions on ligand field theory dealing with the case wherein a luminescent centre is surrounded by multiple kinds of anions. Thus it would need accurate first-principles calculations to compute excited states of rare-earth dopants and hosts quantitatively for realistic models. Although it does not appear facile to perform *ab initio* computations such as GW-method for rare-earth dopants in multinary compounds at present, such high-level and heavy calculations will be good challenges for theoreticians in near future. In the meantime, it seems practical to combine empirical rules with first-principles computation for rational exploration and development of new phosphors, as described in this paper. We expect that the built-up process of *Material Design Concepts* through close collaboration between experiment and theory will promise practical *Crystal-Engineering* to develop new phosphors effectively and efficiently.

Acknowledgments

The authors wish to acknowledge Drs. Toshio Akai, Masaki Takashima, Yutaka Sasaki, Motoyuki Shigeiwa, Kaoru Okamoto and Hiroyuki Imura for analytical investigations for our phosphors. The authors also thank our present/past group members for their assistance for the R&D on our phosphors. The author (MM) gratefully acknowledges Dr. Shinichiro Nakamura for encouragement and continual support for his theoretical works for many years. The neutron diffraction experiment was performed at Japan Atomic Energy Agency. The synchrotron radiation experiments for XAFS were performed at the BL01B1 and BL19B2 of SPring-8 with the approval of the Japan Synchrotron Radiation Research Institute (JASRI).

References

- [1] Mueller-Mach R, Mueller G, Krames M R, Höpfe H A, Stadler F, Schnick W, Juestel T, and Schmidt P 2005 *phys. stat. sol. (a)* **202** 1727
- [2] Watanabe H, Wada H, Seki K, Itou M and Kijima N 2008 *J. Electrochem. Soc.* **155** F31
- [3] Watanabe H and Kijima N 2008 *J. Alloys Compd.* (in press)
- [4] Uheda K, Shimooka S, Mikami M, Imura H and Kijima N 2007 *Proc. 14th International Display Workshops* 899
- [5] Mikami M, Uheda K, Shimooka S, Imura H and Kijima N 2007 *2nd International Symposium on SiAlONs and Non-oxides* (published as Mikami M, Uheda K, Shimooka S, Imura H and Kijima N 2009 *Key Key Eng. Mater.* **403** 11)
- [6] Shimomura Y, Kurushima T, Shigeiwa M and Kijima N 2008 *J. Electrochem. Soc.* **155** J45
- [7] Uheda K, Hirosaki N, Yamamoto Y, Naito A, Nakajima T and Yamamoto H 2006 *Electrochem. Solid-State Lett.* **9** H22
- [8] Uheda K, Hirosaki N and Yamamoto H 2006 *phys. stat. sol. (a)* **203** 2712
- [9] Mikami M, Uheda K and Kijima N 2006 *phys. stat. sol. (a)* **203** 2705
- [10] Dorenbos P 2003 *J. Lumin.* **104** 239
- [11] Dorenbos P 2003 *J. Phys.:Condens. Matter* **15** 4797
- [12] van der Kolk E, Dorenbos P, Vink A P, Perego R C, van Eijk C W E and Lakshmanan A R 2001 *Phys. Rev.* **B64** 195129, and references therein.
- [13] Dorenbos P 2002 *Phys. Rev.* **B65** 235110
- [14] The ABINIT code (URL: <http://www.abinit.org/>) is a common project of the Université Catholique de Louvain, Corning Incorporated, the Université de Liège, the Commissariat à l'Énergie Atomique, Mitsubishi Chemical Corporation, the Ecole Polytechnique Palaiseau and other contributors. Gonze X, Beuken J-M, Caracas R, Detraux F, Fuchs M, Rignanese G-M, Sindic L, Verstraete M, Zerah G, Jollet F, Torrent M, Roy A, Mikami M, Ghosez Ph, Raty J-Y and Allan D C. 2002 *Comput. Mater. Sci.* **25** 478 ; Gonze X, Rignanese G-M, Verstraete M, Beuken J-M, Pouillon Y, Caracas R, Jollet F, Torrent M, Zerah G, Mikami M,

- Ghosez Ph, Veithen M, Raty J-Y, Olevano V, Bruneval F, Reining L, Godby R, Onida G, Hamann D R and Allan D C 2005 *Z. Kristallogr.* **220** 558
- [15] Mikami M, Watanabe H, Uheda K and Kijima N 2008 *Mater. Res. Soc. Symp. Proc.* **1040** Q10-09
- [16] Watanabe H, Yamane H and Kijima N 2008 *J. Solid State Chem.* **181** 1848
- [17] Stadler F and Schnick W 2006 *Z. Anorg. Allg. Chem.* **632** 949
- [18] Kechele J A, Oeckler O, Stadler F and Schnick W 2008 *Solid State Chem.* (in press)
- [19] Li Y Q, Delsing A C A, de With G and Hintzen H T 2005, *Chem. Mater.* **17** 3242
- [20] Barry T L 1968 *J. Electrochem. Soc.* **115** 1181
- [21] Altomare A., Burla M C, Camalli M, Carrozzini B, Cascarano G L, Giacovazzo C, Guagliardi A, Moliterni A G G, Polidori G and Rizzi R 1999 *J. Appl. Cryst.* **32** 339
- [22] Izumi F and Ikeda T 2000 *Mater. Sci. Forum* **321-324** 198
- [23] Parthé E 2006 *Acta Cryst.* **B62**, 335
- [24] Müller U 2007 *Inorganic Structural Chemistry 2nd ed.* (West Sussex: John Wiley & Sons)
- [25] Höpfe H A, Stadler F, Oeckler O and Schnick W 2004 *Angew. Chem. Int. Ed.* **43** 5540
- [26] Stadler F, Oeckler O, Höpfe H A, Möller M H, Pöttgen R, Mosel B D, Schmidt P, Duppel V, Simon A and Schnick W 2006 *Chem. Eur. J.* **12** 6984
- [27] Oeckler O, Stadler F, Rosenthal T and Schnick W 2007 *Solid State Sci.* **9** 205
- [28] Kottaisamy M, Jagannathan R, Jeyagopal P, Rao R P and Narayanan R L, 1994 *J. Phys. D: Appl. Phys.* **27** 2210
- [29] Xie R-J, Hirosaki N and Mitomo M 2007 *Phosphor Handbook 2nd ed.*, ed. Yen W M, Shionoya S and Yamamoto H (Boca Raton: CRC Press)
- [30] Dierre B, Xie R-J, Hirosaki N and Sekiguchi T 2007 *J. Mater. Res.* **22** 1933
- [31] Shimomura Y, Honma T, Shigeiwa M, Akai T, Okamoto K and Kijima N 2007 *J. Electrochem. Soc.* **154** J35
- [32] Wu J L, Gundiah G and Cheetham A K 2007 *Chem. Phys. Lett.* **441** 250
- [33] Newnham R E 2005 *Properties of Materials* (New York: Oxford University Press)
- [34] Philips J C 1973 *Treatise on Solid State Chemistry*, ed. Hannay N B (New York: Plenum Press)
- [35] Kamigaito O and Kamiya N 1998 *Seramikkusu no Butsuri (Physics of Ceramics)* (Tokyo: Uchida Rokakuho Pub.) (in Japanese)
- [36] Okamoto K, Yoshino M, Shigeiwa M, Mikami M, Akai T, Kijima N, Honma T and Nomura M, 2007 *AIP Conference Proceedings* **882** 520